SEMARAK ILMU PUBLISHING

Journal of Advanced Research in Fluid Mechanics and Thermal Sciences

Journal homepage:
https://semarakilmu.com.my/journals/index.php/fluid_mechanics_thermal_sciences/index
ISSN: 2289-7879

Numerical Investigation of Covid-19 Infection Spread Expelled from Cough in an Isolation Ward Under Different Air Distribution Strategies

Ahmed Fahmy El-Haroun[1,*], Sayed Ahmed Kaseb[1], Mahmoud Ahmed Fouad[1], Hatem Omar Kayed[1]

[1] Mechanical Power Department, Faculty of Engineering, Cairo University, Giza, Egypt

ARTICLE INFO

Article history:
Received 11 February 2022
Received in revised form 5 April 2022
Accepted 7 April 2022
Available online 3 May 2022

Keywords:
COVID-19; isolation room; UFAD; particles; air quality; cough

ABSTRACT

COVID-19 is a severe and rapidly spreading respiratory disease that can be transmitted through airborne particles, emitted from cough. This study investigated the influence of underfloor air distribution (UFAD) and overhead air distribution on the diffusion of the coughed particles emitted from two infected patients in an isolation ward. Additionally, the study examined the performance of mounting retractable covers around the exhausts on minimizing the dispersion of the particles. A coupled Eulerian-Lagrangian approach is adopted by using a discrete random walk model. The effect of Brownian force, drag force with Cunningham slip correction factor, turbulence dispersion, Rosin-Rammler, and the breakup is considered in the respiratory airborne coughed particles simulation. The model has a good agreement with the experimental data. The results show that overhead air distribution (case 1) disperses the particles faster to the occupied zone due to the strong mixing between downward inlet airflow and indoor air accompanied by infectious particles. The usage of retractable covers (case 2) significantly minimized the diffusion of the particles inside the ward and their residence time. The particles quantity drops by 53, 98.62, and 99.94 % at 2.0, 10.0, and 120.0 s, respectively, compared to case 1. Case 2 shows the best efficient protection and inhaled air quality for the HCW in all the walking areas inside the room. The upward inlet air in underfloor air distribution (case 3) keeps particles floating for a while at a higher level near the ceiling exhausts, enhancing removal efficiency. Also, it has a slower lateral dispersion of the particles than in case 1. Underfloor air distribution minimized the number of particles by 30.0 % at 120.0 s, compared to overhead air distribution. Inlet air location significantly affects the diffusion of infectious particles in the indoor environment.

1. Introduction

COVID-19 is a very fast-spreading respiratory airborne disease worldwide [1,2]. The spread of the virus caused a very large number of deaths, so countries were forced to apply unprecedented precautionary measures to confront it, such as partial and total closure and sanitary isolation of patients and suspects, in addition to stressing the commitment to social distancing [3,4]. Cough is a respiratory activity that produces a large influx of pathogens with a high initial velocity and causes large diffusion of covid-19 infection. [5].

* *Corresponding author.*
E-mail address: ahmedfahmy@eng.cu.edu.eg

https://doi.org/10.37934/arfmts.95.1.1735

The indoor airflow and ventilation standards significantly affect the dispersion of particles inside the room [6,7]. The risk of infection inside indoor spaces was effectively reduced with increasing ventilation rate and air cleaning capacity [8]. The underfloor air distribution system provides acceptable thermal comfort sensation, energy-saving, and air quality compared with the overhead air distribution system [9–11]. Underfloor air distribution and displacement ventilation are effective in minimizing the dispersion of particles inside the room [12]. In UFAD, the risk of infection increases for the occupants located under the exhausts in the classroom [13]. Abdolzadeh *et al.,* [14] studied the underfloor air distribution in an office room and revealed that seated people close to air supplies were subjected to a high concentration of contaminants. The large droplets pose a great danger to the susceptible person, while the fine droplets are deposited on the walls, floor, and ceiling [15]. The distribution of respiratory particles is effectively controlled by the location of air extraction and ventilation rate [16]. The source of infection and immune patients should be located near the air exhausts and air supplies, respectively [17]. Ventilation effectiveness and particles dispersion are influenced by ventilation rate [18]. Otherwise, the location of air exhausts on the right and left sides of the bed at the lower level provides a reduction in the concentration of the particles in the breathing zone. The exposure to infection for a healthy person can be reduced when using a personal ventilation system of 9 L/s [19]. The work of Zhang *et al.,* [20] revealed that in displacement ventilation, the indoor air distribution and ventilation rate significantly affect the extraction of respiratory droplets compared to inlet air temperature and relative humidity.

The side ceiling ventilation mode provides stratified and lowers the concentration level of particles thus reducing the risk of infection compared with the ceiling ventilation mode [21]. Otherwise, increasing the supply velocity leads to an increase in the mixing process in both modes. The wind speed has a significant effect on locating the risky area [22]. The swirl diffuser of 45° and 60° rotation angles, reduces quickly the amount of inhaled particles in the breathing zone compared with 30° and 90° rotation angles [23]. During coughing, the respiratory airborne infection can travel more than 3.0 m from the infectious person [24]. The evaporation effect can be neglected for particles in the size range of 0.5 to 20 µm [25,26]. For the size of the droplets from 0.1 - 200 µm, the effect of relative humidity on the spread of the droplets can be ignored [27]. The heat of the human body affects the expelled particle's mass and air distribution, and its effect can be neglected on the evaporation rate [28]. Males have a higher initial exhalation velocity than females, so the transmission distance of the respiratory particles is higher for males [29]. The droplets of large diameter dropped to the floor, while the small droplets are suspended in high positions [30]. The fine droplets of a diameter lower than 20 µm disperse with indoor air, while those of a diameter larger than 45 µm are deposited on the surfaces [31]. The initial velocity of coughed droplets varies from 10 to 25 m/s and transmits further than 2.0 m [32]. The transmission distance of the droplets is lower than 2.0 m at a wind speed of 0.0 m/s and can be 6.0 m when the wind speed varies from 4 to 15 km/h. Full-body isopod significantly protects the HCW from the covid-19 virus's infection [33]. Wearing the negative pressure hood for infectious people is effective in preventing the transmission of respiratory airborne droplets [34]. The closer social distance between the infectious person and the healthy one can reduce the spreading of coughed particles in displacement ventilation compared to mixing ventilation [35].

This research concerns the effectiveness of different air distribution strategies on the dispersion of respiratory airborne infection in a COVID-19 densely occupied isolation ward. The laden virus can be transmitted through coughing, so it has been studied as a pathogen. Most of the previous studies focused on one standing or lying patient coughing. Studying the effect of mounting a retractable cover around the exhausts on minimizing the dispersion of infection inside the ward has not been performed elsewhere. Also, no previous studies investigated the effect of underfloor air distribution

on the dispersion of coughed particles from two lying patients inside an isolation ward. The effect of turbulence dispersion, drag force with Cunningham slip correction factor, Brownian force, and the breakup was considered in the respiratory airborne coughed particles simulation. A coupled Eulerian-Lagrangian approach is adopted by using a discrete random walk model for the discrete phase to resolve the effect of turbulent dispersion on particles, and the RANS model for the continuous phase.

2. Mathematical Modelling

2.1 The Eulerian-Lagrangian Approach

A coupled Eulerian-Lagrangian approach is adopted for simulating the distribution of the expelled particles from cough. Where the Eulerian method and Lagrangian discrete phase model are set up for the continuous phase and the dispersion of particles, respectively [36].

2.2 Eulerian-Continuous Phase Equations

The turbulent indoor airflow is modeled using Reynolds-averaged Navier–Stokes equations (RANS), with the standard $k-\varepsilon$ model. The governing equations of mass, momentum, energy, turbulent kinetic energy (k), and turbulence dissipation rate (ε) are solved simultaneously. The standard $k-\varepsilon$ model is preferred due to its suitability for wide ranges of turbulent flows, acceptable accuracy, and computational time efficiency [3,37–43]. Those transport equations are expressed in their general form as follows [44]

$$\frac{\partial \rho(\Phi)}{\partial t} + \nabla.\left(\rho\Phi\vec{V}\right) = \nabla.\left(\Gamma_{\Phi}\nabla\Phi\right) + S_{\Phi} \quad (1)$$

where ρ is the air density, $\vec{V}$ is the velocity vector, Φ is the transported scalar quantity, Γ_{Φ} is the effective diffusion coefficient, and S_{Φ} is the source term.

2.3 Lagrangian Discrete Phase Equations

The particles expelled by cough or sneeze are tracked and simulated using the Lagrangian discrete trajectory model and by solving the force balance equations for droplet motion. The effect of temperature and relative humidity can be ignored on the spread of the particles that have sizes from 0.1 to 200 µm [25–27]. In this study, the size range of the coughed particles is 0.62 - 15.9 µm, with an average diameter of 8.35 µm [45]. Therefore, the evaporation effect was not considered [25,26]. The effect of turbulence dispersion, drag force with Cunningham slip correction factor, Brownian force, and the breakup was considered in the calculation. The stochastic tracking discrete random walk (DRW) model is applied to resolve the influence of turbulence dispersion on particles by integrating the trajectory equations for individual particles [46]. Rosin–Rammler distribution is adopted for the distribution of the coughed particles [1,3,30,47]. The particles start to break up when expelling from the mouth and interact with the indoor air. The breakup model that was used in the simulation is based on Taylor Analogy Breakup (TAB) model [30]. For particles, the lagrangian equations of the motion can be written as follows

$$\frac{dx_{pi}}{dt} = u_{pi} \quad (2)$$

$$\frac{du_{pi}}{dt} = \frac{f_D(u_i - u_{pi})}{\tau_p} + F_{pi} + F_a \quad (3)$$

$$f_D(Re_p) = 1 + 0.15\, Re_p^{0.687} \quad (4)$$

$$Re_p = \frac{\rho\, D_p |u - u_p|}{\mu} \quad (5)$$

$$\tau_p = \frac{\rho_p\, D_p^2\, C_c}{18\,\mu} \quad (6)$$

$$C_c = 1 + \frac{2\lambda}{D_p}\left[1.257 + 0.4\, exp\left(-\frac{1.1\, D_p}{2\lambda}\right)\right] \quad (7)$$

where u is air velocity, u_p is the velocity of droplets, f_D is the Stoke's drag modification function for large particle Reynolds number Re_p, F_{pi} is the gravitational force, τ is droplet's characteristic response time [48], ρ is the air density, ρ_p is droplet's density, C_c is Cunningham slip correction factor, λ is the molecular mean free path and F_{ai} is the additional forces including Brownian force.

3. Model Verification and Validation

3.1 Validation of the Eulerian Model

The Eulerian model has been validated against the experimental work of Yin *et al.,* [49] and the numerical results of Hang *et al.,* [50]. The isolation room geometry as shown in Figure 1 was 4.90 m × 4.32 m × 2.72 m, with a displacement diffuser of 55.0 cm × 70.0 cm × 11.0 cm. The air was exhausted by main and auxiliary grilles with a dimension of 0.254 m × 0.254 m and 0.305 m × 0.254 m, and extracting 36.0 CFM and 78.0 CFM, respectively. The air was supplied at a velocity of 0.14 m/s and a temperature of 19.5 °C. The measurements were conducted on the air velocity (u/u_s) and temperature (θ), where $\theta = (T - T_s)/(T_e - T_s)$, T_e is the main outlet temperature and u_s is the air supply velocity. More details can be found in Yin *et al.,* [49]. As revealed in Figure 2, the present model has a high agreement with the experimental data of Yin *et al.,* [49] and shows a high accuracy compared to the numerical results of Hang *et al.,* [50].

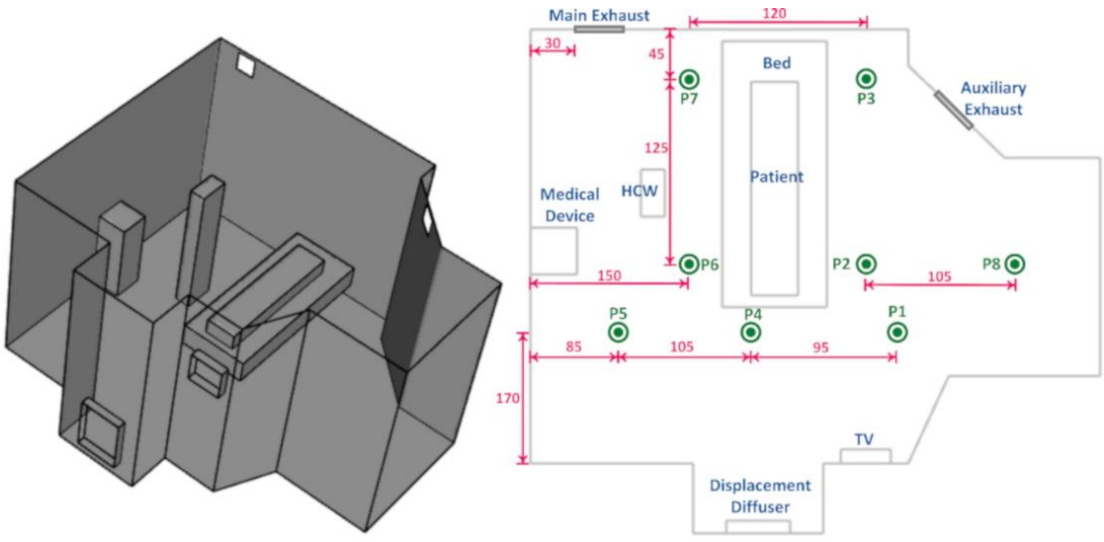

Fig. 1. Configurations of the isolation room (All dimensions are in cm)

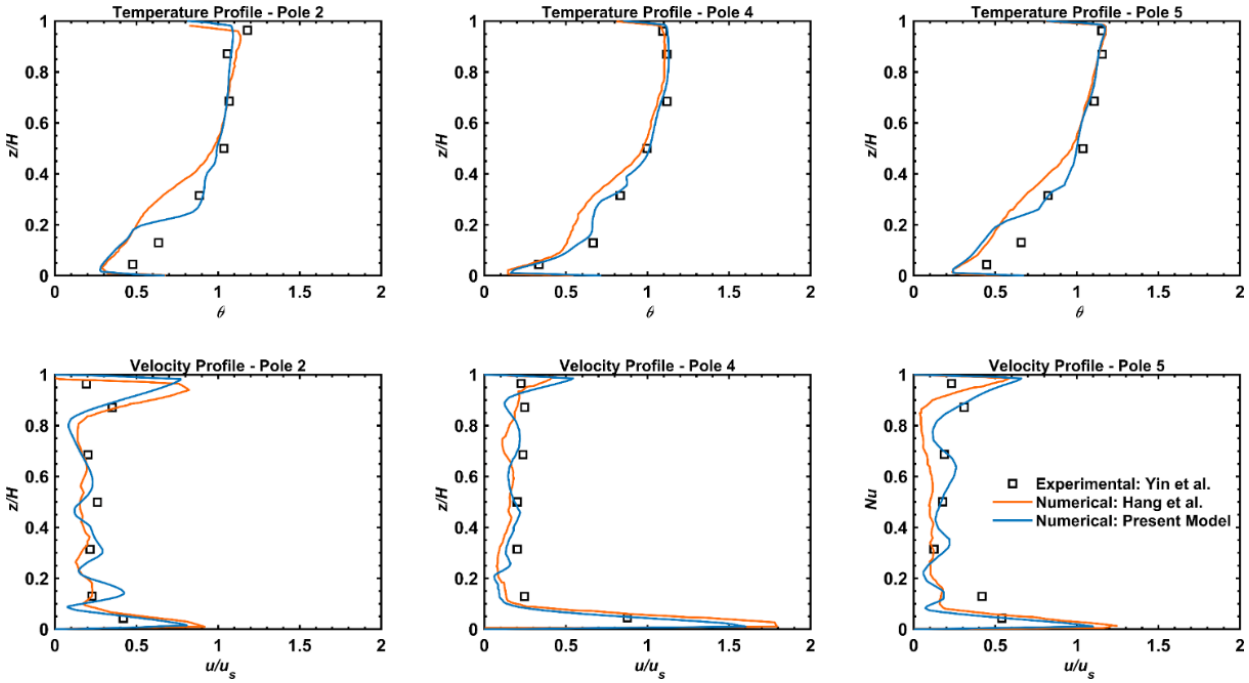

Fig. 2. Comparison between the results of the present model and the numerical results in [50] and the experimental data in [49], z is the vertical distance, and H is the gross room height

3.2 Validation of Particles Dispersion - Lagrangian Discrete Phase

The Lagrangian discrete model has been validated against the experimental data of Lu *et al.,* [51]. The room of the experimental work has dimensions of 5.0 m × 2.4 m × 3.0 m. The room was divided into zones 1 and 2 with an opening of (0.95 m × 0.7 m) in the middle and center of the room as seen in Figure 3(a). The air was supplied with an inlet velocity of 0.09216 m/s in zone 1 and extracted from zone 2 with dimensions (1.0 m × 0.5 m) for both the supply and the exhaust. The particles are uniformly distributed in the room having an initial velocity of zero m/s and then disperse with indoor airflow. The particles have different diameters of 1,2,3,4 and 5 μm. The particles have a density of 865 kg/m^3 and each one has a mass of 147.35 μg. The comparison between the present model and the experimental work of Lu *et al.,* [51] shows a good agreement as seen in Figure 3(b).

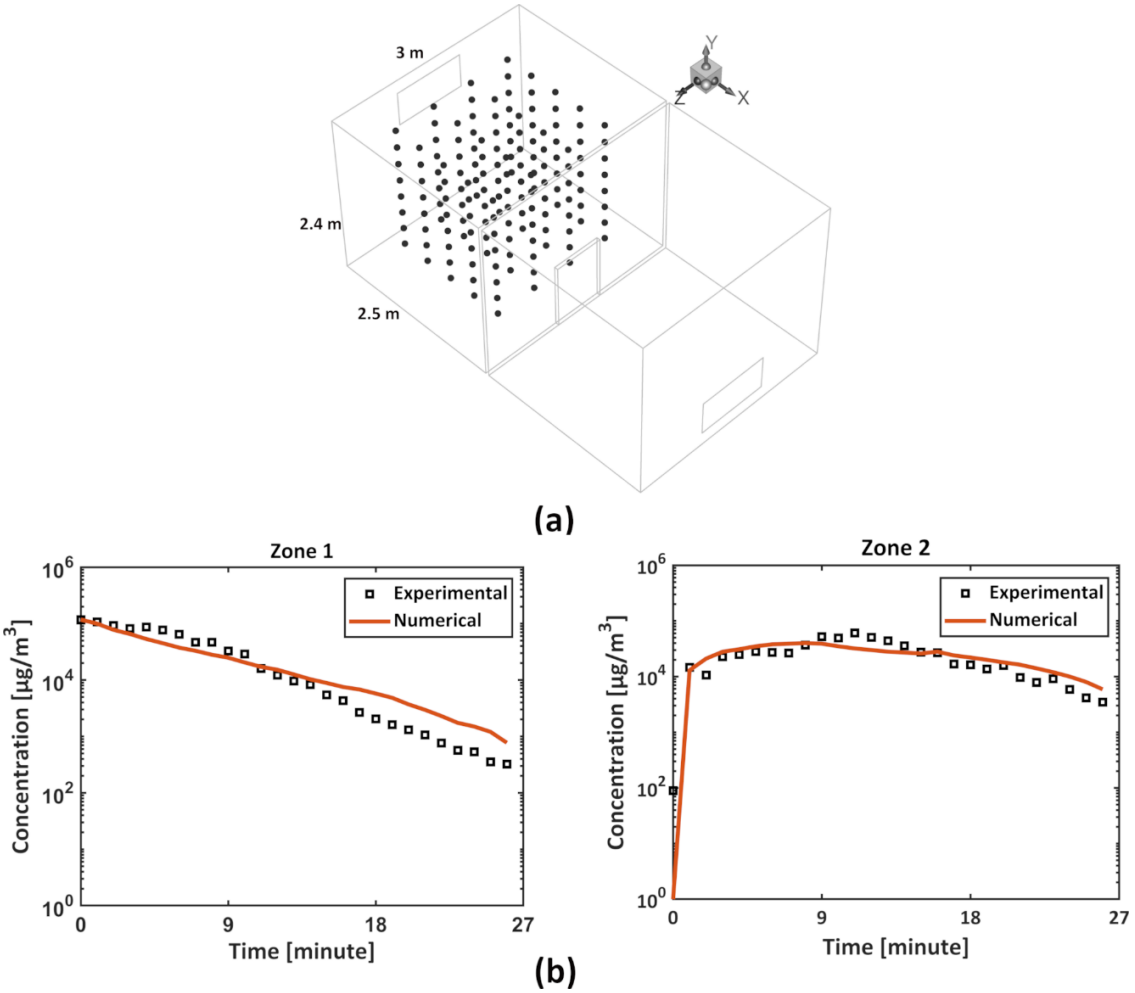

Fig. 3. (a) Room configuration and initial position of the particles, (b) Comparison between results of the present model and experimental data in [51] at zones 1 and 2

4. Numerical Simulation of the Dispersion of Respiratory Aerosols and Coughed Particles

4.1 Isolation Ward Descriptions

The isolation ward has the same geometry as that was in the University of Hong Kong [52]. The ward has dimensions of 6.7 m × 2.7 m × 6.0 m. The ward involves six patients lying in six beds and a standing health care worker. In many kinds of literature, the occupant's body was simulated as a cubical shape of head, chest, arms, and legs to save computational time [17,31,44]. The occupants have a length of 1.70 m. The standing health care worker is located 0.26 m away from the wall behind and in the middle distance between two beds. The six beds are with dimensions (2.0 m × 0.8 m × 0.8 m) and have 1.0 m space in between as shown in Figure 4. The gap between each bed and the wall behind the head is 0.1 m. The head of each patient is 0.2 m away from the wall. For each patient, the mouth is located at 0.98 m from the floor and 0.324 m from the wall behind the bed.

Two air distribution strategies are implemented in the present study as shown in Figure 4. Overhead air distribution is presented in cases 1 and 2, while the underfloor air distribution is presented in case 3. In overhead air distribution (case 1), there are nine downward inlets at the ceiling with a square area (0.6 m x 0.6 m), and six outlets mounted at the walls behind the patients (directly above the patients and 0.15 below the ceiling). Six of the inlets are above the beds and the others are in the middle of the ward. In overhead air distribution (case 2), the air inlets are the same as in case 1. While the six air outlets are mounted above the patient's head on the behind walls at a 1.7 m

distance from the floor. Also, the outlets are surrounded by retractable covers of 0.7 m × 0.5 m x 0.5 (width × height x depth). Each cover has a thickness of 2.0 cm and is centered around the corresponding air exhausts. In underfloor air distribution (case 3), eight inlets are located on the floors with the same dimensions (0.3 m x 0.3 m). The inlets are distributed as four inlets are located in the middle of the ward, while another four inlets are positioned at the sides corners of the ward as seen in Figure 4. Six outlets are located at the ceiling directly above each patient's head. In all cases, exhausts have the same dimensions of 0.3 m × 0.15 m.

In section 5.1, cases 1, 2, and 3 investigate the dispersion of respiratory airborne particles expelled from the cough of two infected patients (patients 2 and 5). **Error! Reference source not found.** summarizes the simulated cases.

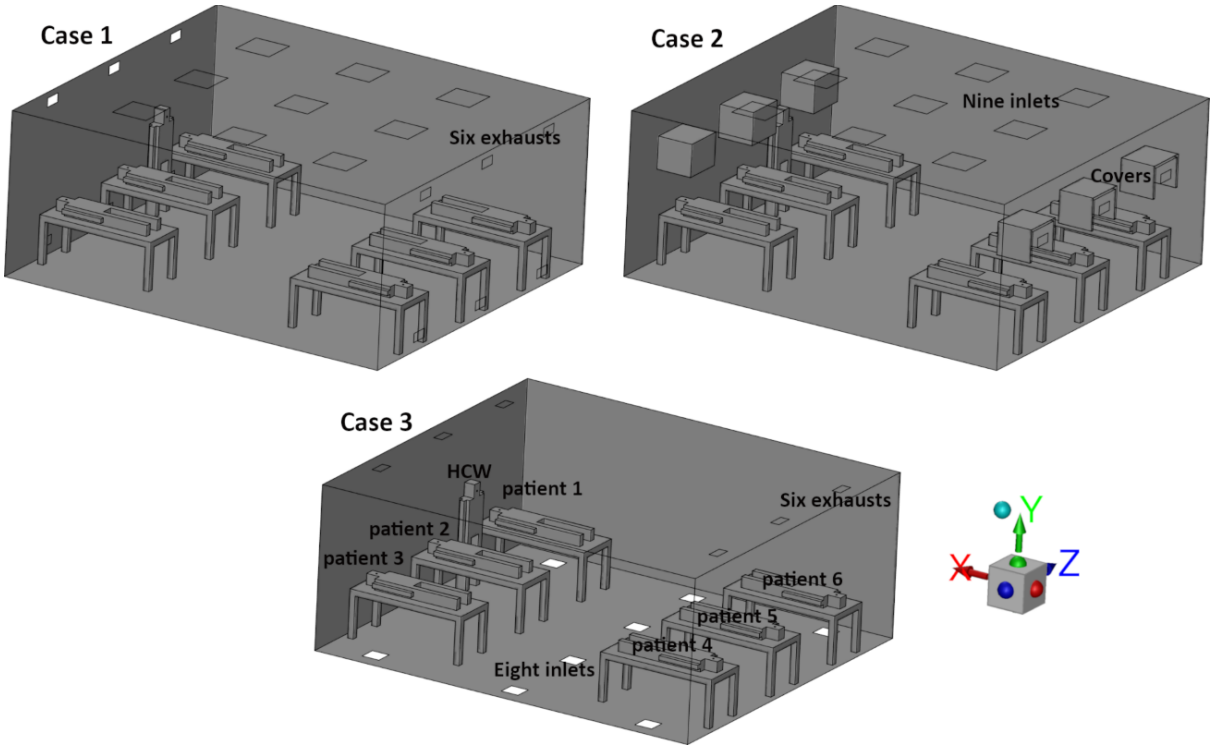

Fig. 4. Simulated isolation ward configurations

Table 1
A list of the simulated cases

Case	ACH	Inlets position	Exhausts position
1	12.9	Ceiling	walls
2	12.9	Ceiling	walls with covers
3	12.9	Floor	ceiling

4.2 Boundary Conditions of the Continuous Phase

The air was supplied into the ward with a ventilation rate of 12.9 which fulfills the requirements for the COVID-19 patient's isolation room [53]. The inlet air has a temperature of 293.0 K. The inlet velocity is 0.12 m/s in overhead air distribution and 0.54 m/s in underfloor air distribution. The mouth has an area of 4.0 cm^2 [54]. The exhaled air from the mouth has a temperature of 308.0 K [3,20,55]. The occupant's surface temperature is kept at 305.5 K. The heat dissipation rate from the ceiling and floor are 16.0 and 5.1 W/m^2, respectively [50], and the walls of the ward are approximated to be

adiabatic walls (adjacent to other spaces at the same interior thermal conditions). A pressure outlet boundary condition is adopted for the exhausts.

4.3 Boundary Conditions of the Dispersion of the Particles

Patients 2 and 5 expelled particles due to cough at the same instant. The single cough has an initial velocity of 10 m/s [12,56] and lasts for 0.5 s [28,44]. The expelled particles have a temperature of 308.0 K [3,20,55]. The coughed particles' size varies from 0.62 to 15.9 µm, with an average diameter of 8.35 µm [45] having a total mass of 6.7 mg [56] and a density of 998.2 kg/m^3 [3]. In the Lagrangian model, air supply and exhaust ports are adopted as an escape boundary condition, and a trap condition is set to the walls, beds, and human body [44]. In addition, The patient's mouth is set up as an escape boundary condition [57]. The transient simulation was solved based on a time step of 0.05 s. Table 2 summarizes the boundary conditions that are set up in the current study.

Table 2
The boundary conditions employed in the present study

Computational domain	6.7 m (x) × 2.7 m (y) × 6.0 m (z)
Air supply ports	V_{in}= 0.12 m/s (overhead air distribution); V_{in}= 0.54 m/s (UFAD); T_{in}= 293.0 K; escape
Air exhausts	Six exhausts; pressure outlet; escape
Patients	Temperature of 305.5 K; no-slip wall boundary; trap
Walls and beds	Adiabatic; no-slip wall boundary; trap
Ceiling and floor	Heat release rates of 16 W/m^2 and 5.1 W/m^2, respectively, trap
Patient's mouth	Mouth area is 4.0 cm^2, escape
Cough	Expelled velocity of 10 m/s; expelled period of 0.5 s
Particles	particles size range 0.62 - 15.9 µm, average diameter of 8.35 µm; total mass of 6.7 mg; density of 998.2 kg/m^3; temperature of 308.0 K

4.4 Mesh and Time Independence Test

The model was developed in ANSYS FLUENT® R2020R1. The SIMPLE algorithm was used as a solver to couple the local pressure and velocity [58,59]. The second-order scheme was used for the spatial discretization of the equations. The simulation of all cases started with a steady RANS simulation until reaching to quasi-steady result. Then, the simulation changed to transient simulation for 120.0 s to simulate the dispersion of the coughed particles. The solution convergence criteria in the steady simulation were taken as 10^{-6} for the energy conservation equation, and 10^{-4} for mass, momentum, k, and ε equations. The mesh is generated using ANSYS Design Modeler® 2020R1 with 7733158 tetrahedral elements. Increasing the number of mesh nodes increases the solution accuracy, as well as the computational costs. So, the numerical solution has been tested using different mesh sizes, as shown in Figure 5, to choose the smallest mesh size at which the solution is independent. The differences between different mesh sizes results show that using the size of 40 mm makes the solution independent of the mesh size with acceptable computational time. A similar test has been performed to choose the time step in transient simulations. three-time step values of 0.1, 0.05, and 0.025 s have been tested where the coughed particles' penetration distance (Y-direction) in case 1 has been monitored at 1.0 and 2.0 s. As shown in Figure 5, there is a clear difference between the time steps of 0.1 and 0.05 s, but the differences between 0.05 and 0.025 s time steps are minimal. Therefore, a 0.05 s time step is adopted for the present transient simulations.

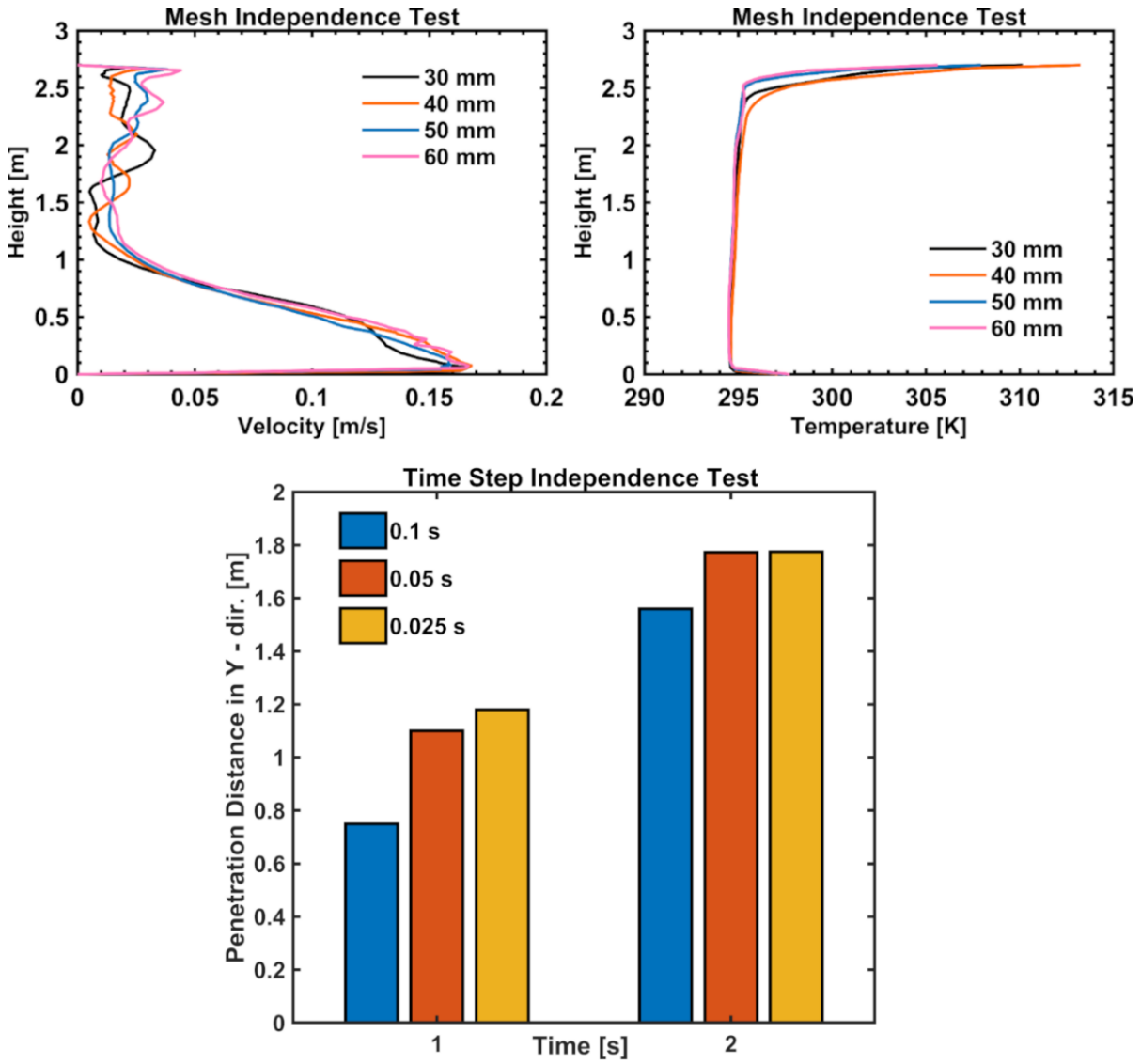

Fig. 5. Mesh and time-step independence tests

5. Results and Discussion

5.1 The Dispersion of Coughed Particles

The coughed particles disintegrate and break up into a wide range of particles size when they are expelled from the mouth and interact with the indoor airflow. Where the large size of the particles was 14.2 µm. Figure 6 shows the evolution of coughed particles dispersion, represented by particles diameter, for 120.0 s from the initiation of cough inside the ward for case 1. The diffusion of the particles is shown at ten different time instants during the time domain. The initial velocity of coughed particles is 10 m/s and the coughing process lasts for 0.5 s. Figure 6(a) shows the coughed particles when reaching the ceiling at 2.0 s. The particles travel upward toward the ceiling and the exhausts form a conical jet under the influence of their momentum. The conical jets slightly bend toward the exhausts due to the draft. The dispersion of the cough by the second patient (on the left) is the same as that of the fifth patient (on the right). At 3.0 s, the low-level particles continue on their way to the ceiling and still maintain their conical shape as in Figure 6(b). The particles start to lose their momentum after accumulation on the ceiling. The particles spread with the ceiling, forming two thick layers adjacent to the ceiling and the wall corner (covering the exhausts) as depicted in Figure 6(c) at 5.0 s. A cluster of the particles is in the vicinity of the edge inlet supplies above the coughing

patients. For the period 2 – 5 s, many particles escaped from the exhausts. Also, another group of particles was deposited on the ceiling and the wall corner.

Over time, the particles lose their velocity and are dominated by indoor air movement, buoyancy, drag, and Brownian motion. The particles that reach the inlet ports are pushed down with the inlet air flow stream to the breathing level above beds as in Figure 6(d) at 10.0 s. Also, particles at the lower level of the layers diffused due to the Brownian and indoor air movement. So far, the area in the middle of the ward between beds is free from the infected particles. At 20.0 s, there are two vertical columns of particles under the inlets and above the infected patients as seen in Figure 6(e). The particles fall on the bed, part of them deposited on the beds and patients' bodies and the others dropped to the floor. It can be noticed that the middle of the ward is a clean area up to 20.0 s. The mixing between the inlet air stream and the indoor air carrying infectious particles causes a great diffusion of the particles. As presented in Figure 6(f) at 30.0 s, the two layers of the particles approach each other near the ceiling at the middle inlets of the ward. Also, the breathing level in the middle region is free from infection. A vertical column of the particles was formed under the middle inlet as cleared in Figure 6(g). There are two circular regions in the middle of the room free from infectious particles at 40.0 s. These zones are located between the rows of the inlet ports. Therefore, the inlet air has a primary role in the spread of the particles. The area of these two regions decreases with the strong mixing between the inlet and indoor air as depicted in Figure 6(h) and (i) at 60.0 s and 80.0 s, respectively. At 120.0 s, these areas are disappeared. The small particles floated at a high level near the ceiling due to buoyancy. Nevertheless, part of the small particles spread in the ward due to the external influence of both inlet airflow stream and indoor air motion. On the contrary, the larger particles are suspended at a level lower than the small particles and deposited on the surfaces. In addition, it was dominated by gravity and the mixing between the inlet and indoor air. Also, it forms a dense cloud in the middle of the ward. The strong mixing between both inlet and indoor air in the occupied area enhances the dispersion of the particles inside the space. Thus, the risk of infection increases as well.

Figure 7 shows the dynamics of coughed particles, represented by particle diameter, inside the ward at a time domain of 120.0 s for case 2. Eight different time shots are displayed to investigate the spread of the particles inside the ward. The location of the inlets is similar to case 1 but the six exhausts are centered at 1.7 m from the floor (on the walls) directly above the patients and surrounded by retractable covers. As shown in Figure 7(a) at 2.0 s, half of the coughed jets are confined inside the covers. The particles still move under their momentum with a complete capture inside the covers as seen in Figure 7(b) at 3.0 s. The covers perform as a trap for the particles. A large number of particles adhered to the inside surfaces of the covers. In addition, many particles are escaped through the exhausts. At 5.0 s, Figure 7(c) shows that a very little amount of particles seeped out from the cover due to gravity for the large particles and Brownian movement for the small particles. The seeped particles lose their momentum inside the cover due to drag. As depicted in Figure 7(d), the particles dropped on the area between the head of patients and the back wall. Their concentration at 10.0 s was lower than in 5.0 s as many of the seeped particles were deposited on the back wall, patients' heads, and beds. Also, a part of these particles is extracted through the exhausts. At 10.0 s, the number of the particles has a great reduction. At 20.0 s as seen in Figure 7(e), a few particles are suspended in the region between the covers and beds, and at the level of the covers. The suspended particles at the breathing level are small particles influenced by buoyancy, whereas the rest between the covers and beds are a cluster of small particles affected by indoor air movement and Brownian motion, and large particles influenced by gravity. The suspended particles between the covers and beds are deposited on the beds and the rest are extracted through the exhausts. Figure 7(f) shows that most of the little suspended particles are light particles at 30.0 s. At

60.0 and 120.0 s, the number of suspended particles is very low approximately twelve particles as seen in Figure 7(g) and (h). The ward at the entire time domain is a clean space from infection. Therefore, the walking spaces for the HCW are free from infection. The risk of infection is excluded. This ensures great protection to the HCW during his motion inside the ward at all instants.

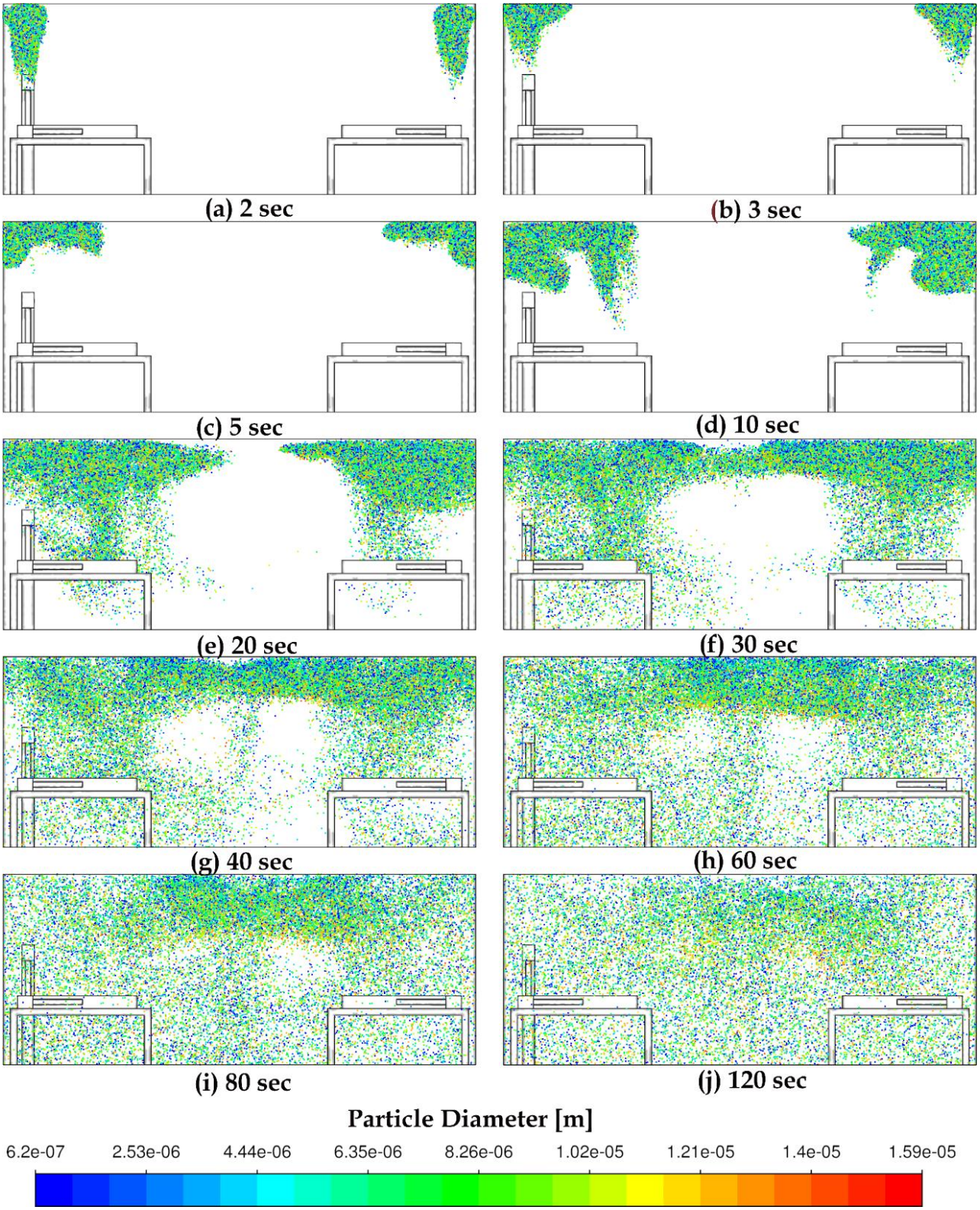

Fig. 6. Evolution of the dispersion of coughed particles in case 1 at (a) 2 s, (b) 3 s, (c) 5 s, (d) 10 s, (e) 20 s, (f) 30 s, (g) 40 s, (h) 60 s, (i) 80 s, (j) 120 s

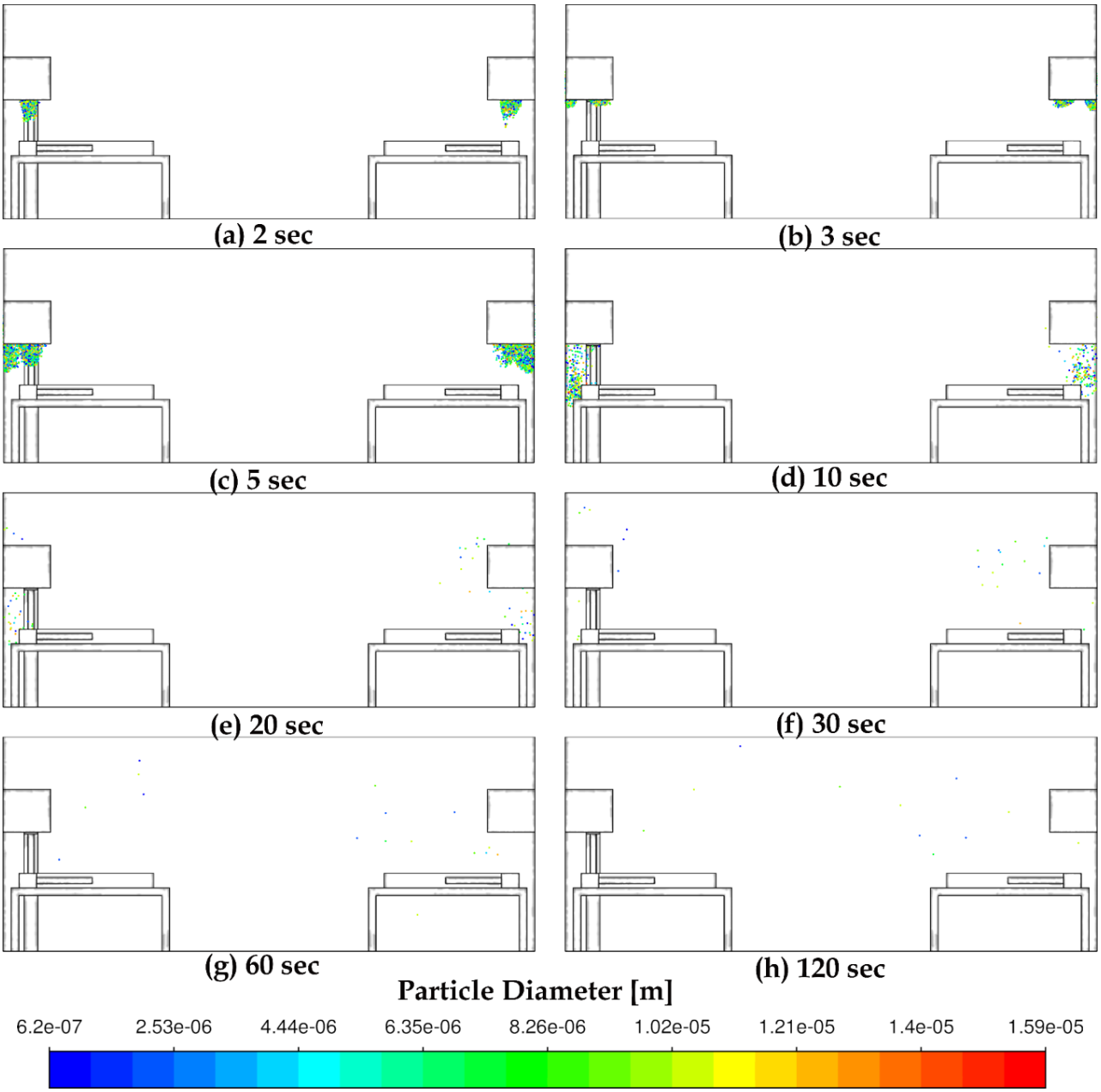

Fig. 7. Evolution of the dispersion of coughed particles in case 2 at (a) 2 s, (b) 3 s, (c) 5 s, (d) 10 s, (e) 20 s, (f) 30 s, (g) 60 s, (h) 120 s

Figure 8 shows the diffusion of cough inside the ward during 120.0 s for case 3. The dispersion of coughed particles is seen at ten instants. As Figure 8(a) at 2.0 s, the expelled particles reached the ceiling under their momentum forming a conical jet. The conical jet in case 3 (see Figure 8(a)) is not bent to the wall corner as in case 1 (see Figure 6(a)) depending on the exhausts' location. The particles are withdrawn through the exhausts and still maintain their conical shape as seen in Figure 8(b) at 3.0 s. The strong draft due to exhausts locations dampens the particles' lateral dispersion with the ceiling. The particles are concentrated at the high left and right corners of the wall as shown in Figure 8(c) and (d) at 5.0 and 10.0 s, respectively. The strong draft and weak mixing at the upper zones limit the particles 'dispersion with the ceiling compared to case 1. At 20.0 s as seen in Figure 8(e), the lateral dispersion of the particles is weak. This dispersion is due to the external influence of indoor air movement, buoyancy, gravity, and Brownian force. As depicted in Figure 8(f), the expelled

particles from the second and fifth patients move slowly to the right and left, respectively, compared to case 1. The large particles dropped due to gravity and indoor air motion, accompanied by light ones as seen in Figure 8(g). Also, the particles from the two patients approach each other at 40.0 s. The occupied zone in the middle of the ward is a clean area free from infection. The light particles float near the ceiling exhausts as they are mainly affected by buoyancy and Brownian force, and the large particles fall due to gravity with clear separation, as shown in Figure 8(h) at 60.0 s. The heavy particles dropped and deposited on the beds and the ground by the effect of gravity as seen at 60.0 and 80.0 s. They are accompanied by a little number of lighter ones. The concentration of the particles in the middle of the ward increases due to the dispersion of indoor air accompanied by infectious particles by inlet airflow as shown in Figure 8(j) at 120.0 s. the upward airflow from the ground dampens the downward motion of the particles. In addition to decreasing the mixing in the upper zone except for overhead air distribution.

Figure 9 represents the number of particles during 120.0 s inside the ward for cases 1, 2, and 3. At 0.5 s (end of cough), the number of particles is the largest. The particles quantity in cases 1 and 3 are identical up to 2.0 s and after that, they differed as seen in Figure 9(a). This is due to that the particles are still on their path to the ceiling and have not yet reached the location of the exhaust. Also, they are far from the surfaces to deposit on. It varied after 2.0 s with a sharp reduction from 2.0-3.0 s, due to the extraction of the particles through the exhausts and deposition on the ceiling. The slope of the reduction in particles quantity in case 3 is larger than in case 1 in the range 2.0-6.0 s and then approximately is the same with monotonically decreasing up to 10.0 s. The largest variation of the number of particles between cases 1 and 3 occurs in the period from 2.0 to 6.0 s. This is due to the strong draft of the exhausts as in case 3, they are located at the ceiling in the direction of the particle's trajectory. Also in these two cases, the slope of particles quantity decreases with time due to the dispersion of the particles inside the ward. Due to a large number of suspended particles in case 1, this slope is slightly larger than in case 3 from 10.0 to 120.0 s as shown in Figure 9(b). The particles quantity in case 3 is lower than in case 1 with a reduction ratio of 32.0 and 30.0 % at 10.0 and 120.0 s, respectively. On the contrary, in case 2 as seen in Figure 9(a), the quantity of the particles has a steeper drop after 1.0 s until 10.0 s due to both the strong extraction through exhausts and the deposition of the particles on the inner surfaces of the covers. At 2.0 s in this case, the quantity of the particles drops 53 %. Case 2 reached the steady-state faster at 10.0 s as depicted in Figure 9(b). The number of particles in case 2 is 713 particles and 12 particles at 20.0 s and 120.0 s respectively. Case 2 has a reduction ratio of 98.62 and 99.94 % at 10.0 and 120.0 s, respectively, compared to case 1.

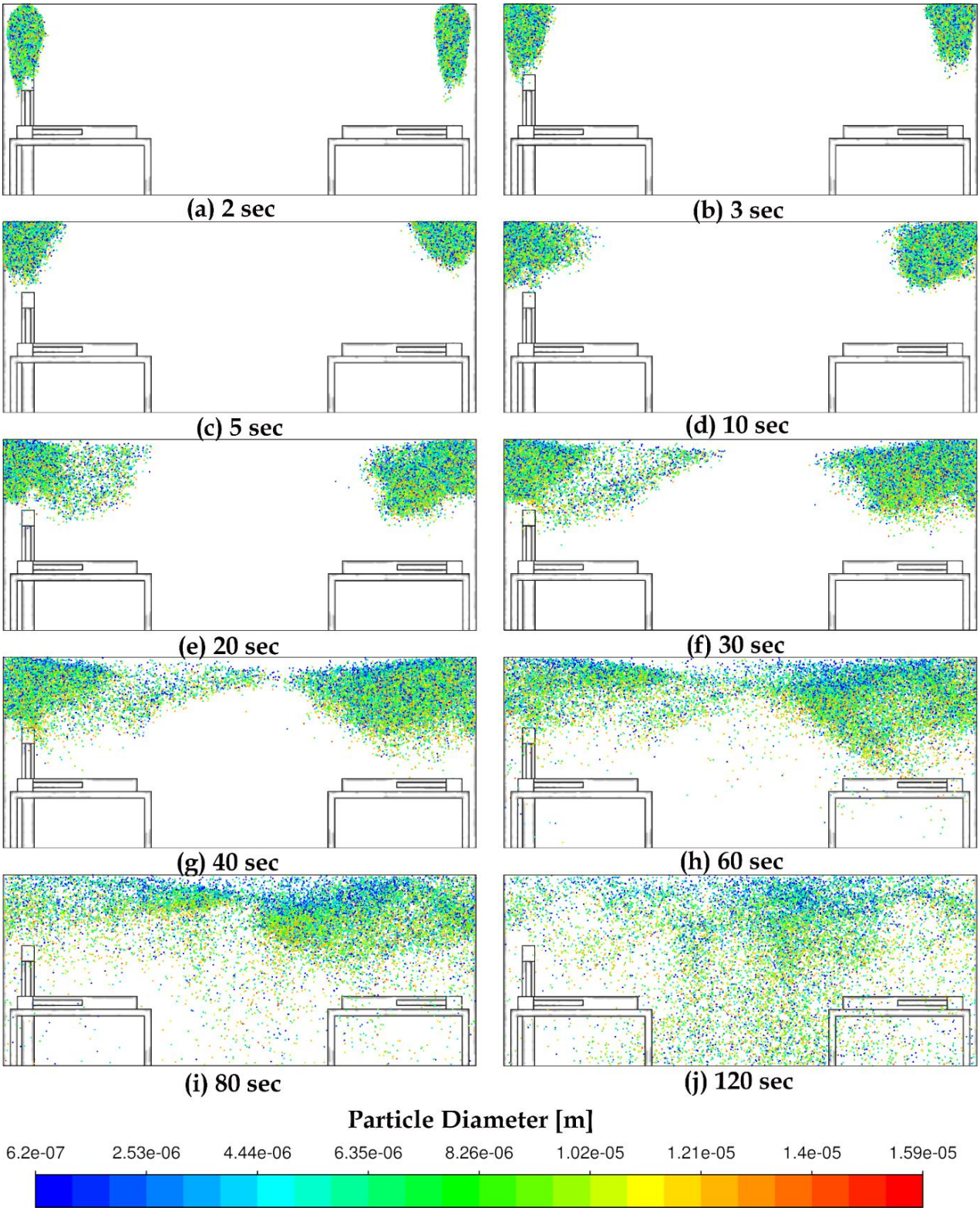

Fig. 8. Evolution of the dispersion of coughed particles in case 3 at (a) 2 s, (b) 3 s, (c) 5 s, (d) 10 s, (e) 20 s, (f) 30 s, (g) 40 s, (h) 60 s, (i) 80 s, (j) 120 s

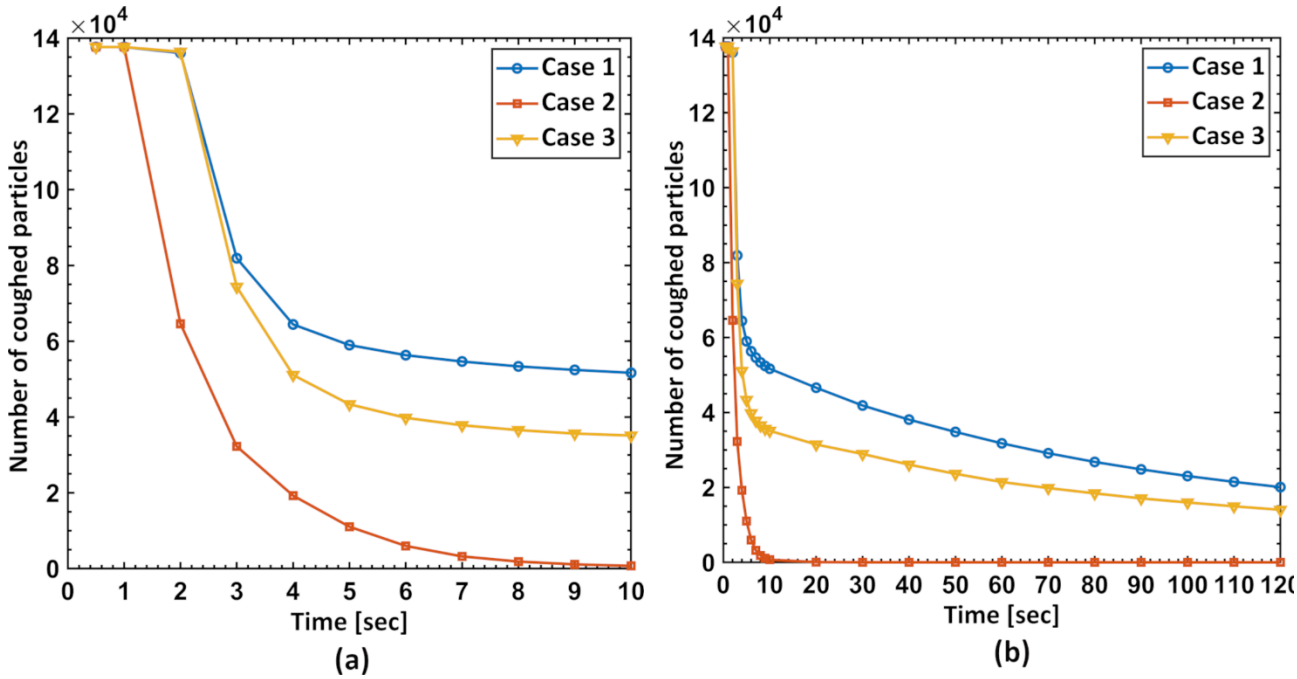

Fig. 9. The number of coughed particles inside the ward for cases 1,2, and 3 versus time (a) 0.5 - 10.0 s range, (b) 0.5 - 120.0 s range

6. Conclusions

This study was conducted in a densely occupied isolation room with six patients, infected with COVID-19, and a standing healthcare worker. The objective was to evaluate the performance of the air distribution systems on the dispersion of the infection inside the ward. In addition to their effectiveness in minimizing the risk of infection for the HCW. The overhead air distribution and underfloor air distribution were studied in the research. The source of infection is two lying patients expelled particles due to cough at the same moment. A coupled Eulerian-Lagrangian approach is adopted by using a discrete random walk model for the discrete phase to resolve the effect of turbulent dispersion on particles, and the RANS model for the continuous phase. Rosin-Rammler distribution was adopted to simulate particles of different sizes. The study took into consideration the influence of turbulence dispersion, breakup, drag force, and Brownian movement. The main findings of the study according to the obtained results were as follow

i. In overhead air distribution (case 1), the strong mixing between the inlet air stream and infectious particles after 5.0 s provides a great diffusion of the coughed particles. Thus, the risk of infection increases. The inlet airflow stream has a primary role in the diffusion of the particles inside the ward.
ii. The location of inlets in overhead air distribution significantly affects the dispersion of infectious particles inside the ward.
iii. In using the retractable covers (case 2), most of the expelled particles were captured by the covers and deposited on their inner surfaces. In addition, a great extraction through the exhausts. All of this causes a steeper drop in the quantity of the suspended particles inside the ward early. It has a 53 % reduction in the quantity of the particles at 2.0 s. Also, the number of particles was minimized by 98.62 and 99.94 % at 10.0 and 120.0 s, respectively, compared to case 1. Therefore, particles have a very low residence time inside the ward.

iv. Developing the overhead air distribution with retractable covers improves the inhaled air quality and minimized the risk of infection to the HCW ensuring great protection.
v. For underfloor air distribution, case 3 has a weak mixing in the upper level, so a large amount of the fine particles was suspended on the upper level except in case 1. In addition, the particles are suspended at a high level for a while before being dropped into the occupied zone in contrast to case 1. The lateral dispersion of the particles in case 3 is slower than in case 2. The middle of the ward was a clean area for 20.0 and 40.0 s in cases 1 and 3, respectively.
vi. The particles are diffused more near the inlet airports in case 3 (UFAD). So it is essential to keep the inlets at a distance from the HCW.
vii. Exhausts located at the ceiling directly above the patient improve removal efficiency.
viii. Case 3 (UFAD) minimized the number of particles by 30.0 % at 120.0 s, compared to case 1.

Acknowledgment
Not applicable.

Funding
This research was not funded by any grant.

References

[1] Dbouk, Talib, and Dimitris Drikakis. "On coughing and airborne droplet transmission to humans." *Physics of Fluids* 32, no. 5 (2020): 053310. https://doi.org/10.1063/5.0011960
[2] World Health Organization. "Novel Coronavirus (2019-nCoV): situation report, 11." (2020).
[3] Portarapillo, Maria, and Almerinda Di Benedetto. "Methodology for risk assessment of COVID-19 pandemic propagation." *Journal of loss prevention in the process industries* 72 (2021): 104584. https://doi.org/10.1016/j.jlp.2021.104584
[4] Dong, Ensheng, Hongru Du, and Lauren Gardner. "An interactive web-based dashboard to track COVID-19 in real time." *The Lancet infectious diseases* 20, no. 5 (2020): 533-534. https://doi.org/10.1016/S1473-3099(20)30120-1
[5] Kähler, Christian J., and Rainer Hain. "Fundamental protective mechanisms of face masks against droplet infections." *Journal of aerosol science* 148 (2020): 105617. https://doi.org/10.1016/j.jaerosci.2020.105617
[6] Jones, Benjamin, Patrick Sharpe, Christopher Iddon, E. Abigail Hathway, Catherine J. Noakes, and Shaun Fitzgerald. "Modelling uncertainty in the relative risk of exposure to the SARS-CoV-2 virus by airborne aerosol transmission in well mixed indoor air." *Building and environment* 191 (2021): 107617. https://doi.org/10.1016/j.buildenv.2021.107617
[7] Mingotti, Nicola, Richard Wood, Catherine Noakes, and Andrew W. Woods. "The mixing of airborne contaminants by the repeated passage of people along a corridor." *Journal of Fluid Mechanics* 903 (2020). https://doi.org/10.1017/jfm.2020.671
[8] Shah, Yash, John W. Kurelek, Sean D. Peterson, and Serhiy Yarusevych. "Experimental investigation of indoor aerosol dispersion and accumulation in the context of COVID-19: Effects of masks and ventilation." *Physics of Fluids* 33, no. 7 (2021): 073315. https://doi.org/10.1063/5.0057100
[9] Nada, S. A., H. M. El-Batsh, H. F. Elattar, and N. M. Ali. "CFD investigation of airflow pattern, temperature distribution and thermal comfort of UFAD system for theater buildings applications." *Journal of Building Engineering* 6 (2016): 274-300. https://doi.org/10.1016/j.jobe.2016.04.008
[10] Ho, Son H., Luis Rosario, and Muhammad M. Rahman. "Comparison of underfloor and overhead air distribution systems in an office environment." *Building and Environment* 46, no. 7 (2011): 1415-1427. https://doi.org/10.1016/j.buildenv.2011.01.008
[11] Lee, Kwang Ho, Stefano Schiavon, Fred Bauman, and Tom Webster. "Thermal decay in underfloor air distribution (UFAD) systems: Fundamentals and influence on system performance." *Applied Energy* 91, no. 1 (2012): 197-207. https://doi.org/10.1016/j.apenergy.2011.09.011
[12] Zhang, Yixian, Guohui Feng, Zhiqiang Kang, Yang Bi, and Yilin Cai. "Numerical simulation of coughed droplets in conference room." *Procedia Engineering* 205 (2017): 302-308. https://doi.org/10.1016/j.proeng.2017.09.981

[13] Cheong, Chang Heon, Beungyong Park, and Seong Ryong Ryu. "Effect of under-floor air distribution system to prevent the spread of airborne pathogens in classrooms." *Case Studies in Thermal Engineering* 28 (2021): 101641. https://doi.org/10.1016/j.csite.2021.101641
[14] Abdolzadeh, Morteza, Ehssan Alimolaei, and Marcelo Pustelnik. "Numerical simulation of airflow and particle distributions with floor circular swirl diffuser for underfloor air distribution system in an office environment." *Environmental Science and Pollution Research* 26, no. 24 (2019): 24552-24569. https://doi.org/10.1007/s11356-019-05651-8
[15] Zhang, Bo, Guangyu Guo, Chao Zhu, and Zhiming Ji. "Transport of aerosol by coughing in an air-conditioned space." In *ASTFE Digital Library*. Begel House Inc., 2019. https://doi.org/10.1615/TFEC2019.hbe.028480
[16] Verma, Tikendra Nath, Arvind Kumar Sahu, and Shobha Lata Sinha. "Study of particle dispersion on one bed hospital using computational fluid dynamics." *Materials Today: Proceedings* 4, no. 9 (2017): 10074-10079. https://doi.org/10.1016/j.matpr.2017.06.323
[17] Satheesan, Manoj Kumar, Kwok Wai Mui, and Ling Tim Wong. "A numerical study of ventilation strategies for infection risk mitigation in general inpatient wards." In *Building simulation*, vol. 13, no. 4, pp. 887-896. Tsinghua University Press, 2020. https://doi.org/10.1007/s12273-020-0623-4
[18] Cho, Jinkyun. "Investigation on the contaminant distribution with improved ventilation system in hospital isolation rooms: Effect of supply and exhaust air diffuser configurations." *Applied thermal engineering* 148 (2019): 208-218. https://doi.org/10.1016/j.applthermaleng.2018.11.023
[19] Xu, Chunwen, Xiongxiong Wei, Li Liu, Li Su, Wenbing Liu, Yi Wang, and Peter V. Nielsen. "Effects of personalized ventilation interventions on airborne infection risk and transmission between occupants." *Building and Environment* 180 (2020): 107008. https://doi.org/10.1016/j.buildenv.2020.107008
[20] Zhang, Yixian, Guohui Feng, Yang Bi, Yilin Cai, Zheng Zhang, and Guangyu Cao. "Distribution of droplet aerosols generated by mouth coughing and nose breathing in an air-conditioned room." *Sustainable Cities and Society* 51 (2019): 101721. https://doi.org/10.1016/j.scs.2019.101721
[21] Xu, Guangping, and Jiasong Wang. "CFD modeling of particle dispersion and deposition coupled with particle dynamical models in a ventilated room." *Atmospheric Environment* 166 (2017): 300-314. https://doi.org/10.1016/j.atmosenv.2017.07.027
[22] Ge, Qinjiang, Xiangdong Li, Kiao Inthavong, and Jiyuan Tu. "Numerical study of the effects of human body heat on particle transport and inhalation in indoor environment." *Building and Environment* 59 (2013): 1-9. https://doi.org/10.1016/j.buildenv.2012.08.002
[23] Taheri, Morteza, Seyed Alireza Zolfaghari, Mahdi Afzalian, and Hassan Hassanzadeh. "The influence of air inlet angle in swirl diffusers of UFAD system on distribution and deposition of indoor particles." *Building and Environment* 191 (2021): 107613. https://doi.org/10.1016/j.buildenv.2021.107613
[24] Lee, Jinho, Danbi Yoo, Seunghun Ryu, Seunghon Ham, Kiyoung Lee, Myoungsouk Yeo, Kyoungbok Min, and Chungsik Yoon. "Quantity, size distribution, and characteristics of cough-generated aerosol produced by patients with an upper respiratory tract infection." *Aerosol and Air Quality Research* 19, no. 4 (2019): 840-853. https://doi.org/10.4209/aaqr.2018.01.0031
[25] Chen, C., and Bin Zhao. "Some questions on dispersion of human exhaled droplets in ventilation room: answers from numerical investigation." *Indoor Air* 20, no. 2 (2010): 95-111. https://doi.org/10.1111/j.1600-0668.2009.00626.x
[26] Morawska, L. J. G. R., G. R. Johnson, Z. D. Ristovski, Megan Hargreaves, Kerrie Mengersen, Shay Corbett, Christopher Yu Hang Chao, Yuguo Li, and David Katoshevski. "Size distribution and sites of origin of droplets expelled from the human respiratory tract during expiratory activities." *Journal of aerosol science* 40, no. 3 (2009): 256-269. https://doi.org/10.1016/j.jaerosci.2008.11.002
[27] Wang, B., A. Zhang, J. L. Sun, H. Liu, J. Hu, and L. X. Xu. "Study of SARS transmission via liquid droplets in air." *Journal of biomechanical engineering* 127, no. 1 (2005): 32-38. https://doi.org/10.1115/1.1835350
[28] Yan, Yihuan, Xiangdong Li, and Jiyuan Tu. "Thermal effect of human body on cough droplets evaporation and dispersion in an enclosed space." *Building and Environment* 148 (2019): 96-106. https://doi.org/10.1016/j.buildenv.2018.10.039
[29] Berlanga, F. A., I. Olmedo, and M. Ruiz de Adana. "Experimental analysis of the air velocity and contaminant dispersion of human exhalation flows." *Indoor Air* 27, no. 4 (2017): 803-815. https://doi.org/10.1111/ina.12357
[30] Chillón, Sergio A., Ainara Ugarte-Anero, Iñigo Aramendia, Unai Fernandez-Gamiz, and Ekaitz Zulueta. "Numerical modeling of the spread of cough saliva droplets in a calm confined space." *Mathematics* 9, no. 5 (2021): 574. https://doi.org/10.3390/math9050574
[31] Ren, Juan, Yue Wang, Qibo Liu, and Yu Liu. "Numerical Study of Three Ventilation Strategies in a prefabricated COVID-19 inpatient ward." *Building and Environment* 188 (2021): 107467. https://doi.org/10.1016/j.buildenv.2020.107467

[32] Zhang, Hualing, Dan Li, Ling Xie, and Yimin Xiao. "Documentary research of human respiratory droplet characteristics." *Procedia engineering* 121 (2015): 1365-1374. https://doi.org/10.1016/j.proeng.2015.09.023
[33] Ramdan, Muhammad Iftishah, Inzarulfaisham Abd Rahim, Nik Hisamuddin Nik Ab Rahman, Ahmad Faizul Hawary, Mohd Azmi Ismail, Mark Selvan, Lim Ban Aik, Alexander Tan Wai Teng, and Lim Wern Pink. "Development Of an Affordable Negative-Pressure Full-Body Isolation Pod for Covid-19 Patient Transportation." *Journal of Advanced Research in Fluid Mechanics and Thermal Sciences* 88, no. 3 (2021): 137-144. https://doi.org/10.37934/arfmts.88.3.137144
[34] Hao, Limei, Jinhui Wu, Jinming Zhang, Zhangyi Liu, Ying Yi, Zongxing Zhang, Enlei Zhang, and Jiancheng Qi. "Development of a negative pressure hood for isolation and transportation of individual patient with respiratory infectious disease." *Biosafety and Health* 1, no. 03 (2019): 144-149. https://doi.org/10.1016/j.bsheal.2019.12.007
[35] Kang, Zhiqiang, Yixian Zhang, Hongbo Fan, and Guohui Feng. "Numerical simulation of coughed droplets in the air-conditioning room." *Procedia engineering* 121 (2015): 114-121. https://doi.org/10.1016/j.proeng.2015.08.1031
[36] Yang, HP, Zhu ZY, Zhou RY, and AB Yu. "Discrete particle simulation of particulate systems: theoretical developments." Chem." *Eng. Sci* 62, no. 13(2007): 3378–3396 https://doi.org/10.1016/j.ces.2006.12.089
[37] Saw, Lip Huat, Bey Fen Leo, Norefrina Shafinaz Md Nor, Chee Wai Yip, Nazlina Ibrahim, Haris Hafizal Abd Hamid, Mohd Talib Latif, Chin Yik Lin, and Mohd Shahrul Mohd Nadzir. "Modeling aerosol transmission of SARS-CoV-2 from human-exhaled particles in a hospital ward." *Environmental Science and Pollution Research* 28, no. 38 (2021): 53478-53492. https://doi.org/10.1007/s11356-021-14519-9
[38] Winata, I. Made Putra Arya, Putu Emilia Dewi, Putu Brahmanda Sudarsana, and Made Sucipta. "Air-Flow Simulation in Child Respirator for Covid-19 Personal Protection Equipment Using Bamboo-Based Activated Carbon Filter." *Journal of Advanced Research in Fluid Mechanics and Thermal Sciences* 91, no. 1 (2022): 83-91. https://doi.org/10.37934/arfmts.91.1.8391
[39] Qing, Nelvin Kaw Chee, Nor Afzanizam Samiran, and Razlin Abd Rashid. "CFD Simulation analysis of Sub-Component in Municipal Solid Waste Gasification using Plasma Downdraft Technique." *Journal of Advanced Research in Numerical Heat Transfer* 8, no. 1 (2022): 36-43.
[40] Widiastuti, Ratih, Juliana Zaini, Mochamad Agung Wibowo, and Wahyu Caesarendra. "Indoor thermal performance analysis of vegetated wall based on CFD simulation." *CFD Letters* 12, no. 5 (2020): 82-90. https://doi.org/10.37934/cfdl.12.5.8290
[41] Caruso, Gianfranco, Matteo Mariotti, and Livio de Santoli. "CFD analysis and risk management approach for the long-term prediction of marble erosion by particles impingement." *CFD Letters* 5, no. 3 (2013): 108-119.
[42] Yohana, Eflita, Aldian Ghani Rahman, Ilham Mile Al'Aziz, Mohamad Said Kartono Tony Suryo Utomo, Khoiri Rozi, Dimaz Aji Laksono, and Kwang-Hwan Choi. "The CFD Application in Analyzing The 024P108 Centrifugal Pump Damage as The Effect of High Vibration using Fluid Flow Discharge Capacity Parameters." *Journal of Advanced Research in Fluid Mechanics and Thermal Sciences* 92, no. 2 (2022): 36-48. https://doi.org/10.37934/arfmts.92.2.3648
[43] Sannad, Mohamed, Youcef Mehdi, Afaf Zaza, Youness El Hammami, Youssef Idihya, and Othmane Benkortbi. "A Numerical Simulation Under Milk Fouling in A Plate Heat Exchanger in The Presence of a Porous Medium." *Journal of Advanced Research in Fluid Mechanics and Thermal Sciences* 91, no. 1 (2022): 1-17. https://doi.org/10.37934/arfmts.91.1.117
[44] Wang, Jinliang, and Tin-Tai Chow. "Numerical investigation of influence of human walking on dispersion and deposition of expiratory droplets in airborne infection isolation room." *Building and Environment* 46, no. 10 (2011): 1993-2002. https://doi.org/10.1016/j.buildenv.2011.04.008
[45] Yang, Shinhao, Grace WM Lee, Cheng-Min Chen, Chih-Cheng Wu, and Kuo-Pin Yu. "The size and concentration of droplets generated by coughing in human subjects." *Journal of Aerosol Medicine* 20, no. 4 (2007): 484-494. https://doi.org/10.1089/jam.2007.0610
[46] Fluent, A. N. S. Y. S. "ANSYS fluent theory guide 15.0." *ANSYS, Canonsburg, PA* 33 (2013).
[47] Pendar, Mohammad-Reza, and José Carlos Páscoa. "Numerical modeling of the distribution of virus carrying saliva droplets during sneeze and cough." *Physics of Fluids* 32, no. 8 (2020): 083305. https://doi.org/10.1063/5.0018432
[48] Lai, Alvin CK, and William W. Nazaroff. "Modeling indoor particle deposition from turbulent flow onto smooth surfaces." *Journal of aerosol science* 31, no. 4 (2000): 463-476. https://doi.org/10.1016/S0021-8502(99)00536-4
[49] Yin, Yonggao, Weiran Xu, Jitendra K. Gupta, Arash Guity, Paul Marmion, Andy Manning, Bob Gulick, Xiaosong Zhang, and Qingyan Chen. "Experimental study on displacement and mixing ventilation systems for a patient ward." *HVAC&R Research* 15, no. 6 (2009): 1175-1191. https://doi.org/10.1080/10789669.2009.10390885
[50] Hang, Jian, Yuguo Li, and Ruiqiu Jin. "The influence of human walking on the flow and airborne transmission in a six-bed isolation room: tracer gas simulation." *Building and Environment* 77 (2014): 119-134. https://doi.org/10.1016/j.buildenv.2014.03.029

[51] Lu, Weizhen, Andrew T. Howarth, Nor Adam, and Saffa B. Riffat. "Modelling and measurement of airflow and aerosol particle distribution in a ventilated two-zone chamber." *Building and environment* 31, no. 5 (1996): 417-423. https://doi.org/10.1016/0360-1323(96)00019-4

[52] Qian, Hua, and Yuguo Li. "Removal of exhaled particles by ventilation and deposition in a multibed airborne infection isolation room." *Indoor air* 20, no. 4 (2010): 284-297. https://doi.org/10.1111/j.1600-0668.2010.00653.x

[53] World Health Organization. *Infection prevention and control during health care when novel coronavirus (nCoV) infection is suspected: interim guidance, 25 January 2020*. No. WHO/2019-nCoV/IPC/2020.2. World Health Organization, 2020.

[54] Gupta, Jitendra K., C-H. Lin, and Q. Chen. "Flow dynamics and characterization of a cough." *Indoor air* 19, no. 6 (2009): 517-525. https://doi.org/10.1111/j.1600-0668.2009.00619.x

[55] Muthusamy, Jayaveera, Syed Haq, Saad Akhtar, Mahmoud A. Alzoubi, Tariq Shamim, and Jorge Alvarado. "Implication of coughing dynamics on safe social distancing in an indoor environment—A numerical perspective." *Building and Environment* 206 (2021): 108280. https://doi.org/10.1016/j.buildenv.2021.108280

[56] Zhu, Shengwei, Shinsuke Kato, and Jeong-Hoon Yang. "Study on transport characteristics of saliva droplets produced by coughing in a calm indoor environment." *Building and environment* 41, no. 12 (2006): 1691-1702. https://doi.org/10.1016/j.buildenv.2005.06.024

[57] Deng, Zhipeng, and Qingyan Chen. "What is suitable social distancing for people wearing face masks during the COVID-19 pandemic?." *Indoor air* 32, no. 1 (2022): e12935. https://doi.org/10.1111/ina.12935

[58] Niknahad, Ali. "Numerical study and comparison of turbulent parameters of simple, triangular, and circular vortex generators equipped airfoil model." *Journal of Advanced Research in Numerical Heat Transfer* 8, no. 1 (2022): 1-18.

[59] Warjito, Warjito, Budiarso Budiarso, Celine Kevin, Dendy Adanta, and Aji Putro Prakoso. "Computational methods for predicting a pico-hydro crossflow turbine performance." *CFD Letters* 11, no. 12 (2019): 13-20. https://doi.org/10.37934/cfdl.12.8.2634